Time-Domain Reflectometry (TDR) monitoring at a lab scale of aerobic biological processes in a soil contaminated by diesel oil

applied sciences

MDPI

Article

Time-Domain Reflectometry (TDR) Monitoring at a Lab Scale of Aerobic Biological Processes in a Soil Contaminated by Diesel Oil

Andrea Vergnano [1,*], Alberto Godio [1], Carla Maria Raffa [2], Fulvia Chiampo [2], Francesca Bosco [2] and Barbara Ruffino [1]

[1] Department of Environment, Land and Infrastructure Engineering, Politecnico di Torino, Corso Duca degli Abruzzi 24, 10129 Torino, Italy; alberto.godio@polito.it (A.G.); barbara.ruffino@polito.it (B.R.)

[2] Department of Applied Science and Technology, Politecnico di Torino, Corso Duca degli Abruzzi 24, 10129 Torino, Italy; s243931@studenti.polito.it (C.M.R.); fulvia.chiampo@polito.it (F.C.); francesca.bosco@polito.it (F.B.)

* Correspondence: andrea.vergnano@polito.it; Tel.: +39-011-090-7737

Received: 6 November 2019; Accepted: 9 December 2019; Published: 13 December 2019

Abstract: This study aims to monitor the biological processes ongoing in a hydrocarbon polluted soil. The experiments were carried out at a laboratory scale by measuring the evolution of its geophysical electromagnetic parameters. Time-domain reflectometry (TDR) probes were used to measure dielectric permittivity and electrical conductivity in columns of sandy soil artificially contaminated with diesel oil (V_{oil}/V_{tot} = 0.19). To provide aerobic conditions suitable for the growth of microorganisms, they were hydrated with Mineral Salt Medium for Bacteria. One mesocosm was aerated by injecting air from the bottom of the column, while the other had only natural aeration due to diffusion of air through the soil itself. The monitoring lasted 105 days. Geophysical measurements were supported by microbiological, gas chromatographic analyses, and scanning electron microscope (SEM) images. Air injection heavily influenced the TDR monitoring, probably due to the generation of air bubbles around the probe that interfered with the probe–soil coupling. Therefore, the measurement accuracy of geophysical properties was dramatically reduced in the aerated system, although biological analyses showed that aeration strongly supports microbial activity. In the non-aerated system, a slight (2%) linear decrease of dielectric permittivity was observed over time. Meanwhile, the electrical conductivity initially decreased, then increased from day 20 to day 45, then decreased again by about 30%. We compared these results with other researches in recent literature to explain the complex biological phenomena that can induce variations in electrical parameters in a contaminated soil matrix, from salt depletion to pore clogging.

Keywords: diesel oil; aerobic biological processes; time-domain reflectometry; dielectric permittivity; electrical conductivity

1. Introduction

Industrial activities have often caused environmental damage to soil and water, with dramatic consequences due to pollutant diffusion along the food chain [1]. Therefore, remediation is one of the pillars to recover the polluted areas and give them back to local communities for safe use. Whatever the remediation method, the monitoring process should be efficient, simple, fast, and possibly low-cost.

In the design of a remediation activity of a wide polluted area, geophysical surveys are often associated with hydrogeological surveys and drilling and coring campaigns, to assess the hydrology, geology, hydrogeological settings, and the contamination level. Nowadays, the main oil clean-up methodologies refer to bioremediation [2], which exploits the activity of microorganisms or plants

to degrade or accumulate pollutants. A previous laboratory-scale study showed that biostimulated indigenous microorganisms can successfully remove diesel oil from soil [3]. During the bioremediation process, biological activity (e.g., generation of by-products, co-metabolites, and biofilms) may induce variations in soil geophysical properties, such as electrical and acoustic impedance [4,5]. Therefore, a time-lapse geophysical investigation could be a useful tool to monitor the biodegradation timeline, but the correlation between the spatial and temporal distribution of geophysical properties and the efficiency of pollutant removal is far from being completely understood [6].

Theoretical models have been proposed to describe the behavior of hydrocarbon fluids in soil and their effects on properties such as dielectric permittivity and electrical resistivity. Endres and Redman [7] developed a pore-scale fluid model for clay-free granular soils. In order to predict the geophysical evidence of a spill of hydrocarbons, Carcione and Seriani [8] proposed a model for the complex permittivity of a soil composed of sandy grains, clay, and silt, partially saturated with gas (air), water, and hydrocarbon based on the self-similar model [9,10]. Thus, multiphase models were implemented such as the Complex Refractive Index Model (CRIM) to predict the dielectric permittivity of a matrix composed of soil, water, gas, and oil. They were validated by using an experimental set based on time-domain reflectometry (TDR) [11], similarly to the approach adopted in our study. These models work well when pollutants displace water contained in soil porosity, as hydrocarbons and water have very different electrical properties. They are less suitable when pollutants displace air because they have relatively similar dielectric permittivity. Hydrocarbon contaminants themselves are a weak source of geoelectrical signals.

Otherwise, it is known that the biological activity associated with degradation generates larger electrical signals than the oil itself. A good correlation between the presence of hydrocarbon contaminants and a substantial increase of the electrical conductivity, caused by microbiological activities, has been reported in previous studies [6,12]; eventually, the long-term degradation of hydrocarbons results in a marked attenuation of electromagnetic signals [13]. A geoelectric survey for the characterization and monitoring of a contaminated site showed an interesting relationship between the production of by-products of biodegradation and the response of induced polarization measurements [6]. Other researchers linked the geophysical investigation of the self-potential response to redox reactions from microbiological activity, developing a "biogeobattery" model [14,15].

The need to control the numerous system parameters of a bioremediation process has suggested developing laboratory-scale experiments. Mori et al. [16] measured the evolution of electrical conductivity in pore water, draining it from contaminated soil microcosms. Masy et al. [17], working on a 2 m^3 tank, compared water monitoring with time-lapse electrical resistivity tomography. Davis et al. [4] observed that biofilm production in biostimulated samples was detectable when measuring a loss of amplitude of the acoustic waves that crossed the system and when observing a peak in imaginary electrical conductivity. A study by Abdel Aal et al. [18] confirmed the relation between peculiar trends in the imaginary part of electrical conductivity and the clogging of pores by biofilms, and also estimated consequent variations of porosity and hydraulic conductivity of soil.

We focus on the geoelectrical properties of soil affected by hydrocarbon contamination, using TDR measurements to provide long-term monitoring of the biological processes in a simple way. Our goal is to validate their use as a support tool for the individuation and characterization of a contaminated area to provide useful information for soil bioremediation applications. Previous works have demonstrated that diesel oil contamination activates the biological processes of degradation by biostimulated indigenous microflora [3,19]. In such a scenario, we prepared two mesocosms, artificially contaminated by diesel oil, and we monitored the electrical properties for more than three months to assess changes in dielectric permittivity and electrical conductivity. The geophysical monitoring was supported by soil sampling in different points of the columns at the end of the test (t = 105 days) to get: diesel oil concentration, viable microbial count, fluorescein diacetate (FDA) analysis, and SEM images.

2. Theoretical Background

2.1. Complex Dielectric Permittivity

The dielectric permittivity (ε) is a physical quantity that describes the ability of a material to oppose an external electric field through the polarization of its molecules. It is often measured in soil, for agronomic or geotechnical purposes, since it is closely related to the water content.

A dielectric material, placed in an electric field, undergoes a polarization phenomenon in which the dipole moment of its molecules aligns according to the external electric field. In this way, a new electric field is generated in the dielectric material, which is opposed to the external one: the greater the permittivity, the greater the opposition to the external electric field and the lower the net field strength [20].

When an electromagnetic wave propagates through a material, for example the soil, an electric field and a magnetic field are generated, oscillating perpendicularly to each other and toward the direction of wave propagation. Its signal is continuously modulated by the soil properties and by the presence of water, changing in amplitude, frequency, and speed. The nature of the material plays a crucial role in defining its behavior when an electromagnetic wave is propagating inside it. For example, while the water particles can rotate and orientate according to the oscillating electric field, those of the soil remain mostly stationary.

The dielectric permittivity ε governs the correlation between the electric field E and the reorganization of electric charges in the material, measured by the electric displacement field D, according to the law:

$$D = \varepsilon E \tag{1}$$

If the electric field is static, and in case of homogeneous and isotropic medium, the dielectric permittivity is constant. Otherwise, in case of an alternate electric field, it depends on the frequency. In case of an anisotropic and non-homogeneous medium, it can change with the spatial coordinates and with the direction.

The dimensionless relative permittivity (or dielectric constant) is defined as:

$$\varepsilon_r = \frac{\varepsilon}{\varepsilon_{vacuum}} \tag{2}$$

The typical values of the relative permittivity are 78.5 for water (at the reference temperature of 25 °C), 1 for air, 2.1 for diesel oil, and about 3–4 for soil grains.

Dielectric permittivity is a complex quantity, and it can be written as the sum of a real component and an imaginary component:

$$\varepsilon_r = \varepsilon_r' + i(\varepsilon_r'' + \frac{\sigma_{dc}}{2\pi f \varepsilon_v}) \tag{3}$$

The real part (ε_r') represents the ability of a medium to store energy in the form of the polarization of molecules. It can be defined considering a parallel plate capacitor: more charge is stored when a dielectric material is put between the plates than if a vacuum is between them. The ratio between the capacitance C (with the material) and C_0 (with vacuum) is the real part ε_r' [21]:

$$\frac{C}{C_0} = \varepsilon_r' \tag{4}$$

The imaginary component of the complex dielectric permittivity is a measure of how much dissipative the material is to an external electric field. The ratio between the imaginary component and the real one is called dissipation factor and its inverse is called quality factor (Q). It is equal to the tangent of δ (δ is the angle between ε_r' and ε_r in the complex plane):

$$\frac{\varepsilon_r'' + \frac{\sigma_{dc}}{2\pi f \varepsilon_v}}{\varepsilon_r'} = tan(\delta) \tag{5}$$

The first term (ε_r'') represents the dielectric losses of the signal due to the vibration or rotation of the molecules. Dielectric losses are frequency-dependent and have a maximum at the so-called relaxation frequency, which for water is 17 GHz at 20 °C [22]: to estimate them, the Debye equation can be used. On the other hand, the second term, characteristic of materials containing free charges, represents the losses due to conductivity [22] and it is dependent on frequency (f) and direct-current (or "zero frequency") electrical conductivity (σ_{dc}). Here, ε_v is the vacuum permittivity.

In the common frequency range of soil sensors (1–1000 MHz), the real part ε_r' is not frequency-dependent while the imaginary component is. However, as they operate at a lower frequency than the relaxation frequency of water, ε_r'' is negligible [23]. Debye relation does not consider conductive losses but only the dielectric mechanism; so, at low frequencies, the imaginary component of dielectric permittivity can be underestimated if conductive losses are not considered (see Equation (3)). According to the literature, conductive losses can be neglected at radar frequencies (10 MHz—2 GHz), because the interfacial and electrochemical mechanisms, such as the surface effects associated with the soil/water interface, are of lower importance [24]. Instead, in the lower MHz range of frequency (<10 MHz) conductive losses are not negligible, so the complex dielectric permittivity depends on particle shape and mineralogy, electrolyte type and concentration, particle orientation, and soil electrolyte interaction [25].

Most soil sensors cannot distinguish between the real and the imaginary component, but they measure a parameter that contains both, called apparent dielectric permittivity (ε_a) [26]:

$$\varepsilon_a = \frac{\left\{1 + \left[1 + tan^2(\delta)\right]^{0.5}\right\}\varepsilon_r'}{2} \quad (6)$$

It is evident from Equations (5) and (6) that high values of ε_r'' or σ_{dc} amplify the ε_a, potentially causing errors in the estimation of soil moisture content. When the ε_r'' values are of the same or lower order of magnitude as ε_r', the ε_a is only minimally affected by the imaginary part. Generally, to solve this problem, soil sensors operate at mid-high frequencies to lower the imaginary component contribute; others measure separately the electrical conductivity at low frequencies to estimate it.

Summarizing this, while the real part is mostly related to moisture content and porosity, the imaginary component is prone to the variability of salinity and temperature, and it depends on interfacial electrochemical mechanisms.

2.2. Models

In soil, water can fill pore spaces with various degrees of saturation, and dielectric constant of this multiphase system is proportional to the percentage of water filling the voids. A simple mathematical model that considers the contributes of every phase was developed by Wharton [27], and it is named CRIM (Complex Refractive Index Model):

$$\varepsilon_b^\alpha = \varepsilon_s^\alpha(1 - \varphi) + [\varepsilon_w^\alpha S_w + \varepsilon_a^\alpha(1 - S_w)]\varphi \quad (7)$$

where φ is the porosity, S is the saturation, and subscripts b, s, w, a refer respectively to bulk, soil grains, water, and air. The exponent α (usually taken $\simeq 0.5$) comes from the relationship between the velocity (v) of an electromagnetic wave and the dielectric constant (ε_r) of the material in which the wave propagates. A simplified form can be:

$$v = \frac{c}{\sqrt{\varepsilon_r}} \quad (8)$$

where c is the light speed. In a medium with high dielectric constant, like water, electromagnetic waves propagate slower than in a low dielectric constant material. The logic of the CRIM model is to calculate

a weighted average of the travel time of a wave passing through its various phases and to relate this time to dielectric permittivity through Equation (8).

2.3. Electrical Conductivity

The electrical conductivity (σ) is related to the imaginary component of dielectric permittivity, according to Equation (3). A conductivity sensor inserted into a soil matrix measures the bulk electrical conductivity dependent on the percentage of the various phases and on the structure itself. An empirical relation between the bulk electrical conductivity and the conductivity of the water solution in soil was suggested by Archie [28]:

$$\sigma_t = \frac{1}{a}\sigma_w \varphi^n S_w^m \quad (9)$$

where n is the cementation exponent, ranging from 1.3 in sand to 2 in consolidated rocks; a is the tortuosity factor or lithologic factor; m is the saturation exponent, equal to 2 in non-polluted soils, up to 3–4 in presence of hydrocarbons. Electrical conductivity is also a complex quantity:

$$\sigma = \sigma' + i\sigma'' \quad (10)$$

As can be observed in Equation (3), σ' (= σ_{dc}), proportional to energy loss per second, is related to the imaginary component of dielectric permittivity (energy loss per cycle). Besides, the imaginary part of electrical conductivity is proportional to the real part of dielectric permittivity [29]:

$$\sigma'' = \omega \varepsilon_r' \quad (11)$$

2.4. Effect of Temperature

Temperature variations can produce effects on dielectric permittivity measures. The dielectric constant of water follows a simple inverse proportionality to temperature, ranging from 88 at 0 °C to 75 at 35 °C, but the temperature calibration to soil moisture measurement is highly soil dependent. Sometimes, the real dielectric can trend upward with increasing temperature, and sometimes downward with increasing temperature [26].

For electrical conductivity a standard temperature calibration can be performed according to the relationship:

$$\sigma_{25\,^\circ C} = \frac{\sigma_T}{[1 + 0.02(T - 25)]} \quad (12)$$

3. Materials and Methods

The study was carried out in two plexiglass columns filled with the same soil and saturated with a water–diesel oil mixture to simulate a contaminated soil. Aerobic conditions were provided by air injection in one of the two mesocosms. Geophysical monitoring was performed by time-domain reflectometry measurements, placing a probe into each column and monitoring the evolution of dielectric permittivity and electrical conductivity. To investigate microbial activity in mesocosms, two analyses were used: FDA hydrolysis and viable microbial count. Samples were also observed with SEM.

3.1. Soil Characterization

The soil used in this project came from a contaminated site near Trecate (Italy). It was collected in a non-contaminated area at a depth of 3 m. It has a neutral pH and it is naturally poor of nutrients. Some characteristic parameters are shown in Table 1 [30]. Analyses were carried out according to the Italian Ministry Decree of 13th September 1999 [31].

Table 1. Results of soil characterization.

Parameter	Value
pH (-)	7.32 ± 0.04
EC (µS/cm) at 25 °C	165 ± 5
Bicarbonate (mg/kg)	66.9 ± 10.8
Ammonia (mg/kg)	2.18 ± 0.11
Nitrate (mg/kg)	68.0 ± 0.4
Chloride (mg/kg)	26.2 ± 0.3
Sulfate (mg/kg)	211 ± 3

3.2. Set-up of Mesocosms

Mesocosms were set-up in sealed Plexiglas columns with diameter of 13.8 cm and filled with 14 cm of soil (soil weight = 3.4 kg). The soil was sieved to obtain a particle size distribution between 0.15 and 2 mm, as described in [32], and it was compacted to reach a uniform porosity of approximately 0.4.

The contamination was simulated adding 0.24 kg of diesel oil to each soil sample (70 g of diesel oil/kg of soil). Moisture content was fixed at 20% V/V, obtained by using a Mineral Salt Medium for Bacteria (MSMB) [33]. The main characteristics of mesocosms are shown in Table 2.

Table 2. Main characteristics of mesocosms.

Parameter	Value
Diameter of columns (cm)	13.8
Soil mass (kg)	3.4
Soil particle size (mm)	0.15–2
Porosity (−)	0.4
Volumetric water content (V/V)	0.20
Volumetric diesel content (V/V)	0.19
C/N ratio (W/W)	450

One of the two columns was connected to a forced-air system and air was injected from the bottom to the top. In the first month of the experiment, aeration was carried out once a week, providing 2 dm^3 of air in 2 min. After 40 days, the second part of the experiment started, with daily aeration of about 20 dm^3 per day. Eventually, at t = 50 days, the forced aeration was stopped.

The aerated column was also inoculated with diesel-degrading microorganisms in order to have an initial concentration equal to 1.25×10^3 colony-forming units (CFU) per gram of soil.

In the other column, only natural aeration due to air diffusion through the soil itself was done. This column was considered the control mesocosm [34].

3.3. Time-Domain Reflectometry

Time-domain reflectometry determines the dielectric permittivity in soil. A TDR probe is composed of a couple of parallel rods linked to a voltage generator and an oscilloscope. An electromagnetic wave is generated and the signal runs along the length of the probe, being reflected when it reaches the end. The time a wave needs to run along a rod is inversely proportional to the bulk dielectric permittivity ε_r', according to Equation (8). The result is an average value of permittivity of the sensed volume; generally, the first centimeters near the sensor are the most influent, although, theoretically, the electromagnetic field propagates indefinitely. Some studies have also tried to analyze in more detail the reflected signal of a TDR measurement to identify zones with different permittivity situated along the length of the rods [35]. A piece of advice from all manufacturers is to pay attention in ensuring that the rods of TDR sensors have good contact with the soil; if air gaps are present around the rods, the sensibility of the instrument is drastically reduced. Summarizing this, water content is efficiently measured by a TDR probe that evaluates the real component of complex dielectric permittivity. Other properties,

like salinity, mostly influence the imaginary component and, consequently, the electrical conductivity. These sensors were selected for their ability to simultaneously measure dielectric permittivity and electrical conductivity, and to provide a temperature correction of measurements.

The TDR probes, as explained in Equation (6), measure an apparent dielectric permittivity because they are sensitive to soil properties linked to the imaginary part of dielectric permittivity. To calculate the real part, they measure, independently from ε_r' measurement, the voltage attenuation of a known non-polarizing waveform at 100 kHz. This voltage ratio ranges from 1 in non-conductive media to about 17 in highly conductive media. The voltage ratio is correlated to the electrical conductivity, which is linked to the imaginary component of the dielectric permittivity through Equation (3). It is assumed that at 100 kHz the imaginary component only represents losses due to conduction phenomena and, therefore, the dielectric losses (ε_r") are negligible.

The probe, manufactured by Campbell Scientific (model: CS 655), composed of two 12-cm long rods, was inserted vertically into the soil. The measurements gave average values of the sensing volume of the probe. The recording was performed every 10 min along the entire duration of the experiment (105 days). A simple scheme of the acquisition instruments is shown in Figure 1.

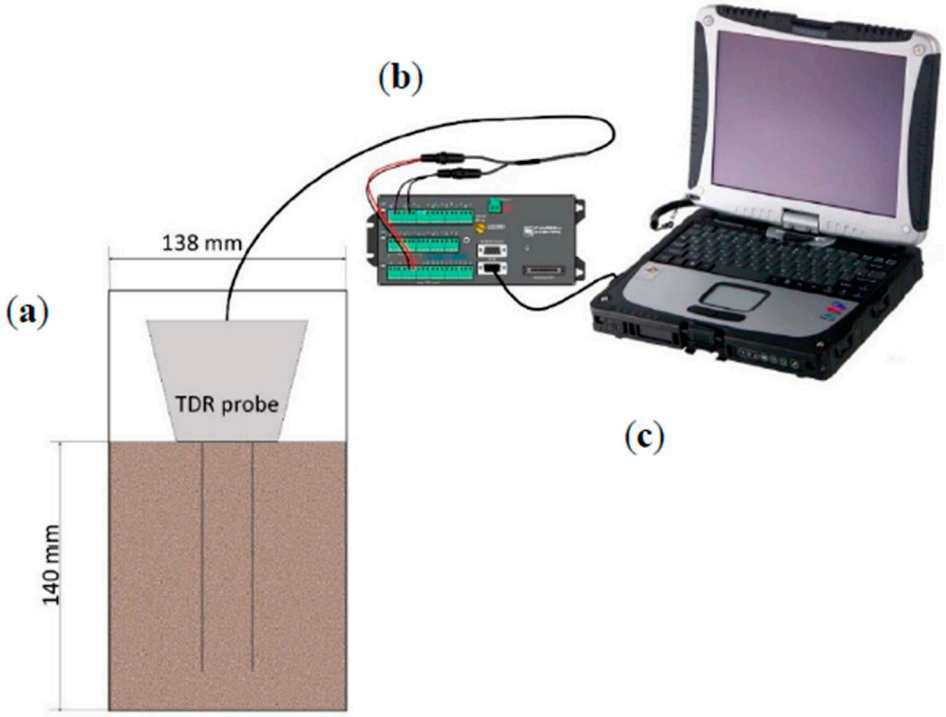

Figure 1. Scheme of time-domain reflectometry (TDR) acquisition set-up. (**a**) Soil column with the TDR probe; (**b**) data-logger; (**c**) external PC for data processing.

3.4. Sampling

Soil sampling of mesocosms was performed at the end of the experiment (t = 105 days). Samples were collected at a depth of 2 cm from the surface, in the middle (8 and 10 cm from the surface), and at the bottom of the columns (depth = 14 cm).

3.5. FDA Analysis

Fluorescein diacetate is a compound that can be hydrolyzed by several enzymes, like protease, lipase, and esterase. The hydrolysis product is fluorescein, characterized by a strong yellow color and, therefore, easily detected by spectrophotometry. In this way, an overall estimation of microbial activity can be obtained.

Methodology reported by Schnurer and Rosswall [36] and modified according to Adam and Duncan [37] was used. Two solutions were used:

- Potassium phosphate buffer—8.7 g/L of K_2HPO_4 and 1.3 g/L of KH_2PO_4. The solution pH is 7.57, which falls within the acceptable range to get the FDA hydrolysis reaction, namely between pH 7–8;
- FDA stock solution in acetone at a concentration of 2 g/L.

Samples of 2 g of soil (on a wet basis) were mixed with 15 mL of phosphate buffer and 100 µL of FDA stock solution in acetone. Each sample was agitated at 50 rpm for 1 h. Then, to stop the hydrolysis reaction, 15 mL of acetone were added. Subsequently, the samples were centrifuged at 6000 rpm for 5 min and then filtered through a 1.2 µm filter to remove any colloidal particles. Absorbance was measured by spectrophotometry at 490 nm. Two replicas were prepared for each sample and one blank containing only the potassium phosphate solution.

A series of samples at known concentrations of pure fluorescein (dissolved in potassium phosphate buffer) was prepared to obtain a calibration line that correlated the absorbance measured with the spectrophotometer with the quantity of fluorescein diacetate hydrolyzed by the enzymatic activity of microorganisms.

3.6. Microbial Counts

For each sample, 50 mg of soil was inserted into a Petri plate under a biological safety cabinet, adding and mixing 100 µL of sterile water. Then, 40 µL of diesel oil was filtered at 0.22 µm and dispersed on the opposite part of the plate. Eventually, MSMB solution with Agar gelling agent (20 g/L), previously sterilized in autoclave, was added. The results are expressed as number of colony-forming units (CFU) per gram of soil.

3.7. Diesel Oil Extraction and Gas Chromatograph Analysis

For each sample, 2 g of contaminated soil was placed in a glass tube with 2 g of anhydrous sodium sulfate, necessary for dehydration, and 30 mL of solvent (acetone and hexane in ratio 1:1 V/V).

The extraction was performed according to EPA method 3546 [38] (moisture 15–30%).

At the end of the extraction, the sample was filtered through a sodium sulfate bed and then through a 0.45 µm nylon filter. A sample of 1 µL was analyzed in a gas chromatograph column according to the EPA method 8015 [39].

4. Results

4.1. Microbial Activity

The number of CFU/g of soil and the fluorescein (µg/g of soil) produced by FDA hydrolysis are shown in Figures 2 and 3, respectively.

4.2. SEM Images

Images of the soil, acquired with scanning electron microscope, are shown in Figures 4–6. Figure 4 shows an SEM image of a sample taken from the surface of the aerated column, in which rod-shaped microorganisms are visible (length is 2–6 µm and diameter is 0.5–1µm).

In the contaminated samples, soil grains were covered by an organic coating, probably due to diesel presence; vice versa, the coating was absent in the non-contaminated samples of the same soil. Figures 5 and 6 show this difference.

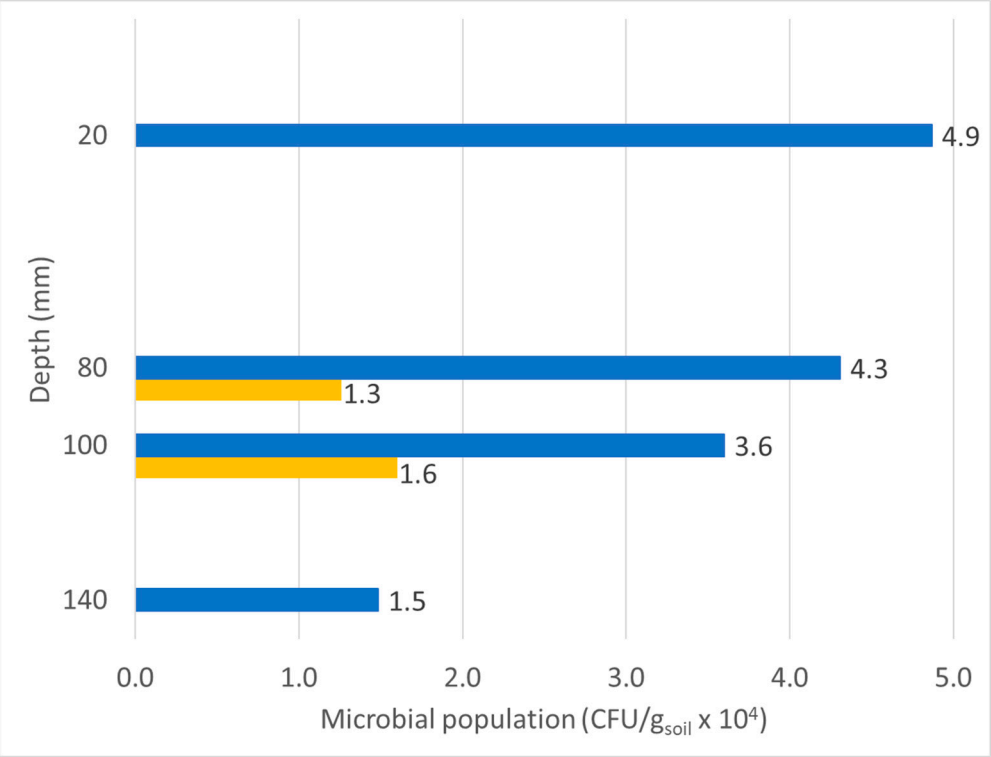

Figure 2. Microbial diesel-degrading population in the mesocosms (CFU/g of soil). Blue: forced aeration mesocosm. Yellow: control mesocosm. Initial microbial concentration in forced aeration mesocosm is 1.25×10^3 CFU/g of soil.

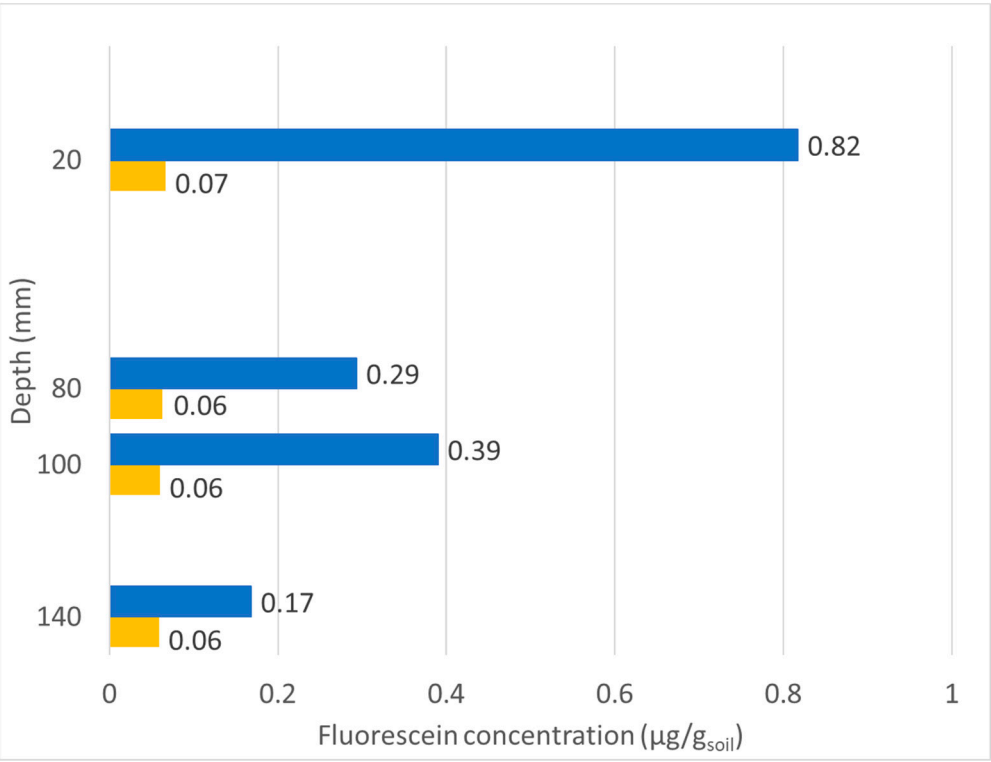

Figure 3. Concentration of fluorescein produced in the mesocosms (µg/g of soil). Blue: forced aeration mesocosm. Yellow: control mesocosm.

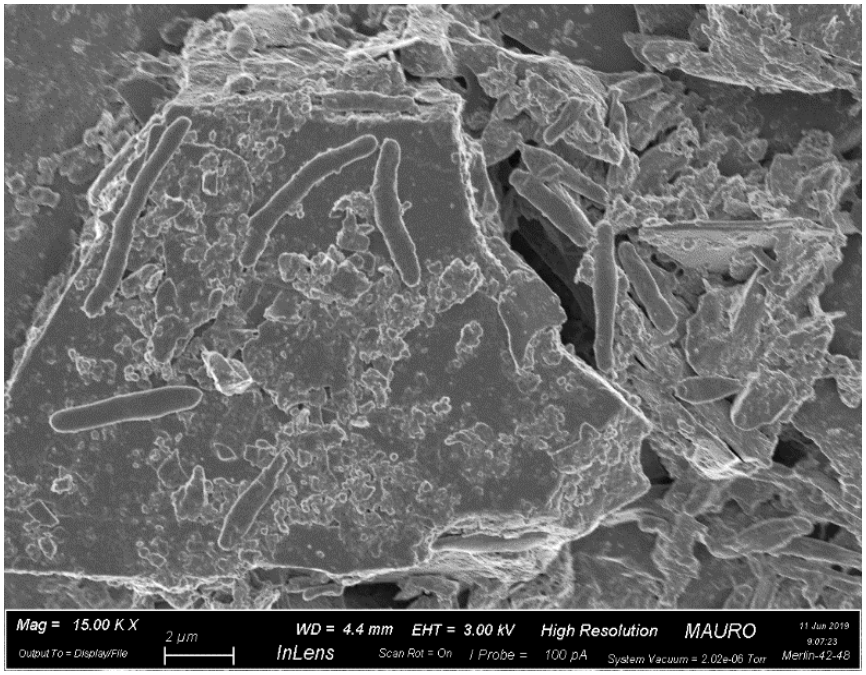

Figure 4. SEM image of soil from the surface of aerated mesocosm. Magnification: 15,000×.

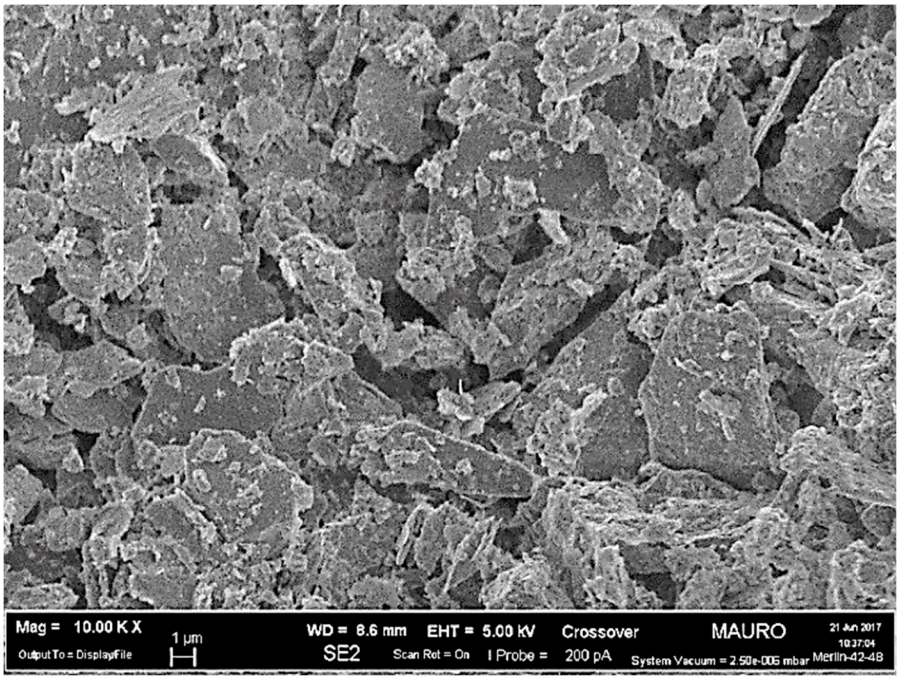

Figure 5. SEM image of non-contaminated soil. Magnification: 10,000×.

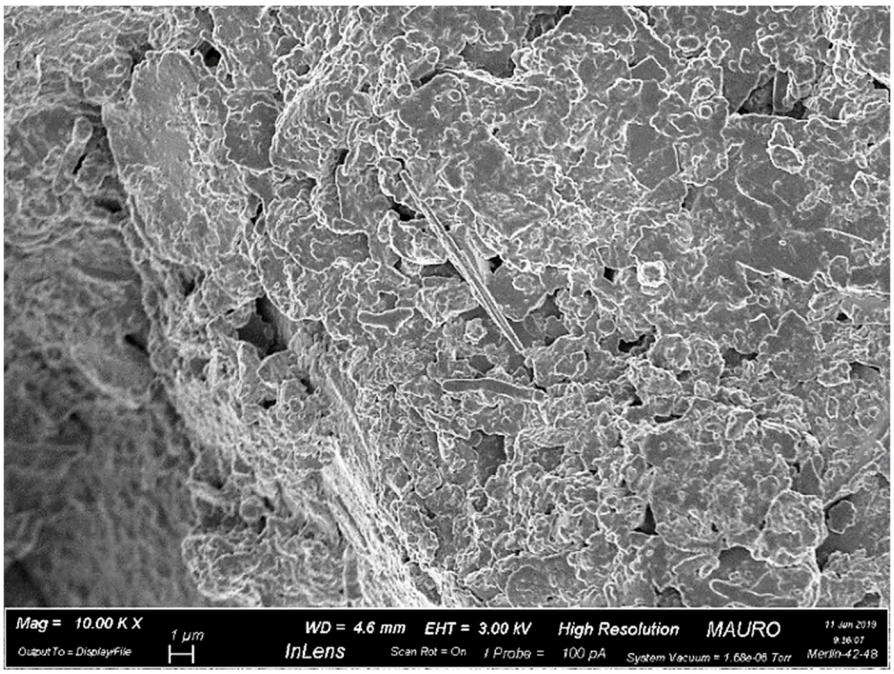

Figure 6. SEM image of aerated column sample (bottom). The diesel coating is evident. Magnification: 10,000×.

4.3. Gas Chromatographic Analysis

The data of the diesel oil concentration at the top, middle, and bottom of each column after 105 days are reported in Figure 7.

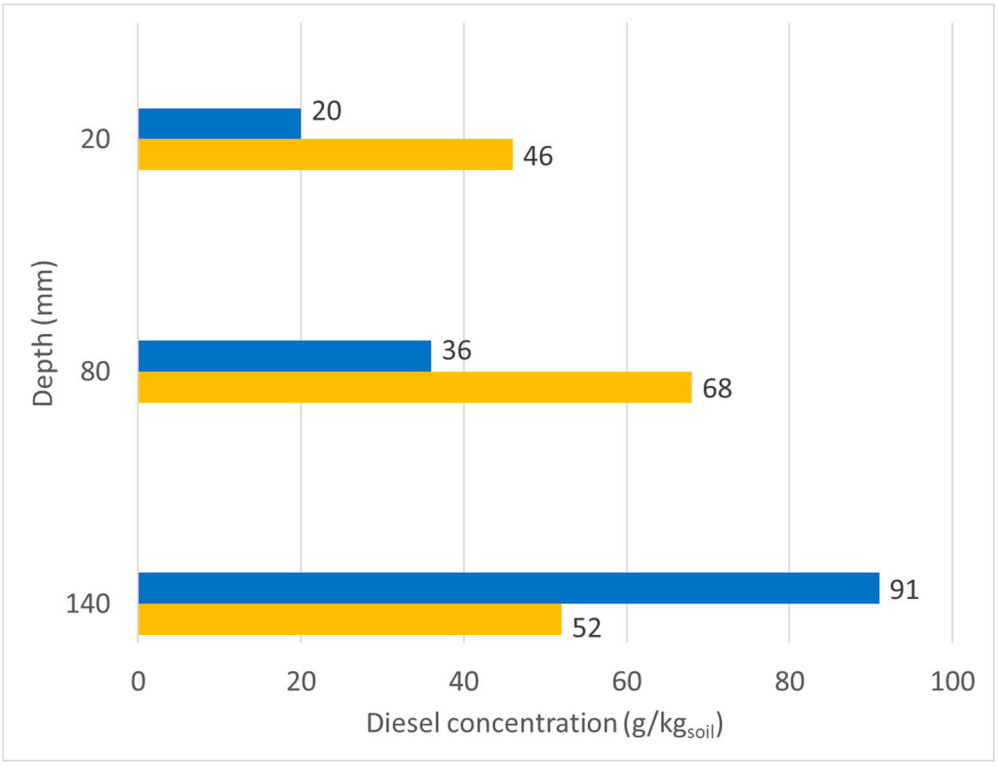

Figure 7. Blue: diesel oil concentration in aerated column. Yellow: diesel oil concentration in control column, t = 105 days.

4.4. TDR Measurements of Geoelectrical Properties

Figures 8 and 9 show the dielectric permittivity and electrical conductivity obtained by 105 days of measurements with TDR probes.

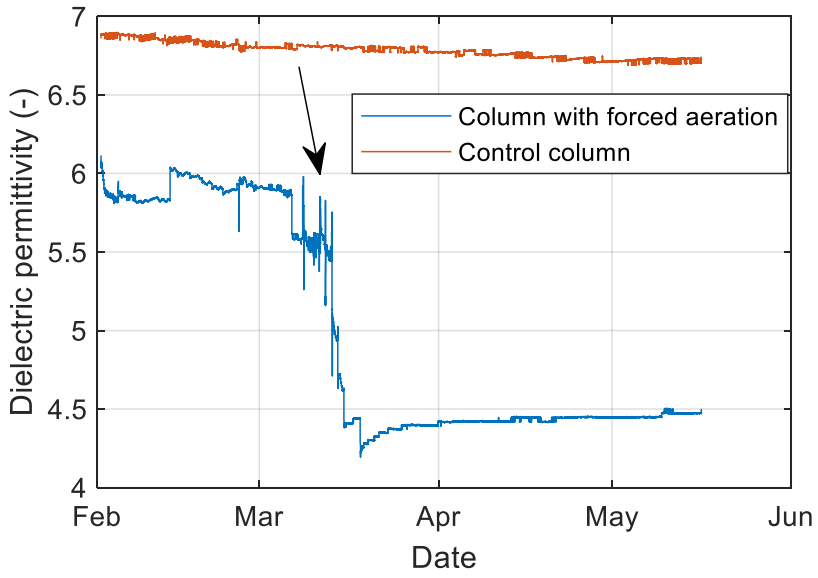

Figure 8. Dielectric permittivity in the mesocosms. Arrow indicates the beginning of daily air injection.

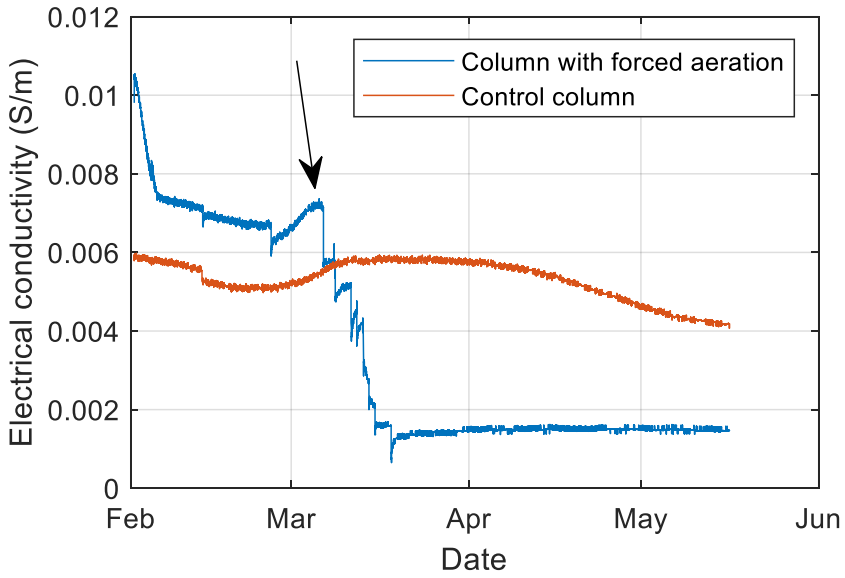

Figure 9. Electrical conductivity with temperature correction in the mesocosms (S/m). Temperature ranged from 15 to 20 °C during the experiment. Arrow indicates the beginning of daily air injection.

5. Discussion

The diesel concentration, from the initial value of 70 g/kg of soil (that corresponds to a volumetric diesel content of 0.19), evolved differently in the two mesocosms (Figure 7). At the 105th day, in the control mesocosm, the diesel oil floated mainly in the middle of the column (68 g/kg of soil), while values of about 50 g/kg of soil were reported at the surface and at the bottom. Observing the walls of the control column, we noticed that a small number of air bubbles was trapped in the porosity of the soil. They may have not allowed proper movement of liquid fluids toward the bottom. In the aerated column, a greater displacement of oil was evident. At the surface, the diesel concentration was measured to be about 20 g/kg of soil, while most of the contaminant was collected at the bottom,

with values above 90 g/kg of soil. We explained this evidence assuming that the air injection produced a great mixing of water and oil at the bottom of the system and had the secondary effect of letting the bubbles of air escape toward the top. The number of samples did not cover the whole depth of the column with adequate spatial discretization to estimate if the monitored biological processes caused also a removal of hydrocarbons.

Anyway, if we consider the results of the biological activity, it is realistic to assume that, at least in the aerated system, a process of degradation occurred because, in previous research, on the same soil and in similar conditions, degradation of diesel compounds was quantitatively estimated [3]. In fact, the microbial population of the mesocosm with aeration and inoculum was significantly higher than that of the natural aeration column (Figure 2). An evident stratification was also observed: near the surface, the number of microorganisms was very high, up to 5×10^4 CFU/g of soil, that decreased going toward the bottom of the column (about 1.5×10^4 CFU/g of soil) against initial population due to inoculum equal to 1.25×10^3 CFU/g of soil. The microbial community distribution was confirmed by FDA analyses, as shown in Figure 3. In the control column, the microbial population along the depth of the column was fairly uniform (about 1.5×10^4 CFU/g of soil) and similar in value to that of the bottom of the aerated column. FDA again confirmed these results.

The SEM images agreed with the microbial counts and FDA analyses. In the aerated column, the quantity of microorganisms at the surface was observed to be qualitatively higher than that at the middle and the bottom of the column, and higher than that of the control column samples (Figures 4 and 6).

The dramatic change in geoelectrical parameters, measured after a month, is caused by the aeration. In the first month, when aeration was applied once a week, some perturbation in the trend of the monitored parameters was observed (Figures 8 and 9). Since t = 40 days, the air was injected once a day, and the airflow provided a stronger perturbation to the measurements. We assumed that, locally around the probes, the porosity increased due to the channeling of the air fluxes, creating additional pores that altered the coupling between the probe and the soil. For this reason, at t = 50 days we decided to stop the air injection. However, in the following days, the electrical conductivity and dielectric permittivity did not return to the initial values and a gap between the previous measurements and the subsequent ones was still very evident. The system did not manage to refill the voids created by air injection and the coupling was spoiled irreversibly.

Regarding the control column, a slight and constant decrease of the dielectric permittivity was observed (Figure 8). Applying the CRIM model, we noted that the changes of the dielectric permittivity can be justified by a loss of about 9% of diesel oil, or about 3% of water (α calibration exponent = 0.4); moreover, it can be supposed that the slow and constant decrease of the dielectric permittivity was caused by displacement of fluids, or by the progressive pore clogging due to the coating of grain particles caused by organic matter. This latter phenomenon was also reported by Mori et al. [16].

The electrical conductivity has a more interesting trend (Figure 9). After an initial decrease, the electrical conductivity increases until the second half of March (t = 50 days). Then, it gradually decreases till the end of the experiment, namely from 0.006 S/m to 0.004 S/m. The observed values of conductivity could be justified, according to the Archie model, by a decrease in water content from 0.2 to 0.175 (about 13%), but this explanation is not consistent with the dielectric permittivity measurement. The electrical conductivity variations are probably due to other phenomena as variations in salinity, for instance, which is one of the most important parameters that influence the electrical conductivity. As the evolution of electrical conductivity in soil is strictly connected to the modifications in the chemistry of the pore water, the initial decrease of this parameter could be due to the progressive depletion of nutrient salts present in MSMB solution used to stimulate bacterial activity. Anyway, the Archie model takes into account the electrolytic conductivity phenomena only; this cannot explain the overall variations of the observed changes in the conductivity. At a later stage of the experiment, the observed increase of the bulk conductivity is reported also by Atekwana et al. [40] and Masy et al. [17]. They linked this effect to an enhanced biological activity, which probably led to the production of acids as co-metabolites,

or as products of the dissolution of CO_2 in water. Then, the consequent acidification of pH could dissolve some inorganic salts present in the soil, causing an increase of salinity in the pore water and therefore in the electrical conductivity. Studies at field-scale showed that bacterial mineralization of organic compounds augments CO_2 in the aquifer and produces organic acids that increase mineral weathering [41].

The last part of the plot shows a decrease in bulk conductivity; this was observed after about 45 days, and it was noticed also in other studies. The study by Mori et al. [16] found a similar electrical conductivity trend, with a peak at about 30 days and then a decrease by doing measurements in the leachate produced in the process. Masy et al. [17] worked at bigger scale (2 m^3), monitoring separately the soil electrical resistivity and the fluid electrical resistivity for 100 days. The most interesting result was that, after 50 days, the microbial degradation activity induced an increase in fluid conductivity; meanwhile, the bulk electrical conductivity decreased, unexpectedly. The authors assumed that significant production of hydrophobic secondary metabolites occurred. To validate this assumption in our experiment, we performed a peak analysis of the gas chromatograms; however, we did not observe any peak that could be evidence of the secondary production of organic compounds.

The TDR technology combines the measurement of the dielectric permittivity, related to the propagation of the electromagnetic field, the polarization of molecules, and the measurement of electrical conductivity, which refers to signal attenuation due to charge movement. The integration of electrical conductivity and dielectric permittivity is, therefore, suitable for the characterization of hydrocarbon-contaminated areas because it can detect ongoing biological processes. Therefore, it could be applied as a time-lapse monitoring tool during a bioremediation campaign. According to our knowledge, time-domain reflectometry measurements have been used in few studies to detect the presence of contaminants: a leakage of hydrocarbons that displaces the water fluid provokes a decrease in the parameters measured with TDR [11,42]. However, we did not find any research about the connection of these measurements to biodegradation activity.

6. Conclusions

We focused on a laboratory experiment to check the reliability of integrated monitoring of dielectric permittivity and electrical conductivity of biological processes in contaminated soil. We understood that the TDR probes can provide very useful data related to ongoing biochemical phenomena. The main challenges were concerned with the complexity of the phenomena that can produce variations of electrical parameters of soil. According to the literature, they can be the removal of diesel oil, the effects of movement and displacement of fluids, the changes in pore water salinity, and the progressive clogging of pores. The air injection into the mesocosms to stimulate the aerobic processes provided a marked effect on the coupling between the probe and the soil in an irreversible way, making measurements unrealistic. Biological analysis, though, confirmed that aeration improves greatly microbial activity and population.

A future experiment will scale-up the mesocosms to bigger columns. The moisture content will be changed to have unsaturated conditions and better natural aeration through the porosity of the soil. Also, by field-scale studies, it is well-known that most biological degradation happens in the vadose zone. Air injection will not be carried out, even if it is strongly suggested to enhance aerobic bioremediation, to avoid soil-probe decoupling. Besides, a system with the addition of nutrient salts will be compared to a system with the addition of water only to better understand the role of salinity in the evolution of the bioremediation processes. Eventually, more in-depth research will be done about variations in the electromagnetic parameters of water due to its electrochemical adhesion to the surface of the soil grains, with the use of other instruments as open-ended coaxial probes.

Author Contributions: Conceptualization, A.G. and F.C.; methodology, A.G., F.C., F.B., and B.R.; software, A.V.; validation, A.G. and F.C.; data curation, A.V., C.M.R., and F.C.; writing—original draft preparation, A.V.; writing—review and editing, A.V., A.G., and F.C.; supervision, F.C. and F.B.; project administration, F.C.; funding acquisition, F.C.

Funding: This research was funded by the project "Geophysical Methods to Monitor Soil Bioremediation", funded by the Italian Ministry of Foreign Affairs and International Cooperation in the frame of the Executive Programme of Scientific and Technological Cooperation between the Republic of India and the Italian Republic for the years 2017–2019 (significant research).

Acknowledgments: We want to personally thank Diego Franco for helping us in the set-up of mesocosms, for his kind contribution to the project, and for his very helpful ideas.

Conflicts of Interest: The authors declare no conflicts of interest.

References

1. Capcarova, M.; Slamecka, J.; Jurcik, R.; Sladecek, T.; Gren, A.; Argente, M.J.C.; Massanyi, P. The occurrence and dynamics of polychlorinated hydrocarbons in roe deer (Capreolus capreolus) in South-western Slovakia. *J. Environ. Sci. Health Part A* **2019**, *54*, 603–607. [CrossRef] [PubMed]
2. Fernando, E.Y.; Keshavarz, T.; Kyazze, G. The use of bioelectrochemical systems in environmental remediation of xenobiotics: A review. *J. Chem. Technol. Biotechnol.* **2019**, *9*, 2070–2080. [CrossRef]
3. Bosco, F.; Casale, A.; Mazzarino, I.; Godio, A.; Ruffino, B.; Mollea, C.; Chiampo, F. Microcosm evaluation of bioaugmentation and biostimulation efficacy on diesel-contaminated soil. *J. Chem. Technol. Biotechnol.* **2019**. [CrossRef]
4. Davis, C.A.; Pyrak-Nolte, L.J.; Atekwana, E.A.; Werkema, D.D., Jr.; Haugen, M.E. Acoustic and electrical property changes due to microbial growth and biofilm formation in porous media. *J. Geophys. Res.* **2010**, *115*, G00G06. [CrossRef]
5. Álvarez, M.; Ruberto, L.; Balbo, L.; Cormack, M. Bioremediation of hydrocarbon-contaminated soils in cold regions: Development of a pre-optimized biostimulation biopile-scale field assay in Antarctica. *Sci. Total Environ.* **2017**, *591*, 194–203. [CrossRef]
6. Arato, A.; Wehrer, M.; Birò, B.; Godio, A. Integration of geophysical, geochemical and microbiological data for a comprehensive small-scale characterization of an aged LNAPL-contaminated site. *Environ. Sci. Pollut. Res.* **2014**, *21*, 8948–8963. [CrossRef]
7. Endres, A.L.; Redman, D.J. Modeling the electrical properties of porous rocks and soils containing immiscible contaminants. *J. Environ. Eng. Geophys.* **2009**, 105–112. [CrossRef]
8. Carcione, J.M.; Seriani, G. An electromagnetic modelling tool for the detection of hydrocarbons in the subsoil. *Geophys. Prospect.* **2000**, *48*, 231–256. [CrossRef]
9. Feng, S.; Sen, P.N. Geometrical model of conductive and dielectric properties of partially saturated rocks. *J. Appl. Phys.* **1985**, *58*, 3236–3243. [CrossRef]
10. Sen, P.N.; Scala, C.; Cohen, M.H. A self-similar model for sedimentary rocks with applications to the dielectric constant of fused glass beads. *Geophysics* **1981**, *46*, 781–795. [CrossRef]
11. Comegna, A.; Coppola, A.; Dragonetti, G.; Sommella, A. Dielectric response of a variable saturated soil contaminated by Non-Aqueous Phase Liquids (NAPLs). *Procedia Environ. Sci.* **2013**, *19*, 701–710. [CrossRef]
12. Cassiani, G.; Binley, A.; Kemna, A.; Wehrer, M.; Flores Orozco, A.; Deiana, R.; Boaga, J.; Rossi, M.; Dietrich, P.; Werban, U.; et al. Noninvasive characterization of the Trecate (Italy) crude-oil contaminated site: Links between contamination and geophysical signals. *Environ. Sci. Pollut. Res.* **2014**, *21*, 8914–8931. [CrossRef] [PubMed]
13. Godio, A.; Arato, A.; Stocco, S. Geophysical characterization of a non-aqueous-phase liquid-contaminated site. *Environ. Geosci.* **2010**, *17*, 141–162. [CrossRef]
14. Revil, A.; Mendonc, C.A.; Atekwana, E.A.; Kulessa, B.; Hubbard, S.S.; Bohlen, K.J. Understanding biogeobatteries: Where geophysics meets microbiology. *J. Geophys. Res.* **2010**, *115*, G00G02. [CrossRef]
15. Atekwana, E.A.; Slater, L.D. Biogeophysics: A new frontier in Earth science research. *Rev. Geophys.* **2009**, *47*, RG4004. [CrossRef]
16. Mori, Y.; Suetsugu, A.; Matsumoto, Y.; Fujihara, A.; Suyama, K. Enhancing bioremediation of oil-contaminated soils by controlling nutrient dispersion using dual characteristics of soil pore structure. *Ecol. Eng.* **2013**, *51*, 237–243. [CrossRef]
17. Masy, T.; Caterina, D.; Tromme, O.; Lavigne, B.; Thonart, P.; Hiligsmann, S.; Nguyen, F. Electrical resistivity tomography to monitor enhanced biodegradation of hydrocarbons with Rhodococcus erythropolis T902.1 at a pilot scale. *J. Contam. Hydrol.* **2016**, *184*, 1–13. [CrossRef]

18. Abdel Aal, G.Z.; Atekwana, E.A.; Atekwana, E.A. Effect of bioclogging in porous media on complex conductivity signatures. *J. Geophys. Res.* **2010**, *115*, G00G07. [CrossRef]
19. Bosco, F.; Casale, A.; Chiampo, F.; Godio, A. Removal of Diesel Oil in Soil Microcosms and Implication for Geophysical Monitoring. *Water* **2019**, *11*, 1661. [CrossRef]
20. Ledieu, J.; De Bidder, P.; De Clerck, P.; Dautrebande, S. A method of measuring soil moisture by time-domain reflectometry. *J. Hydrol.* **1986**, *88*, 319–328. [CrossRef]
21. Keysight Technologies. *Basic of Measuring the Dielectric Properties of Materials*; Application note; Keysight Technologies: Santa Rosa, CA, USA, 2019; literature number: 5989-2589EN.
22. Kaatze, U.; Uhlendorf, V. The dielectric properties of water at microwave frequencies. *Z. Phys. Chem.* **1981**, *126*, 151–165. [CrossRef]
23. Hilhorst, M.A. A pore water conductivity sensor. *Soil Sci. Soc. Am. J.* **2000**, *64*, 1922–1925. [CrossRef]
24. Knight, R.; Endres, A. A new concept in modeling the dielectric response of sandstones: Defining a wetted rock and bulk water system. *Geophysics* **1990**, *55*, 586–594. [CrossRef]
25. Rinaldi, V.A.; Francisca, F.M. Impedance analysis of soil dielectric dispersion (1 MHz–1 GHz). *ASCE J. Geotech. Geoenviron. Eng.* **1999**, *125*, 111–121. [CrossRef]
26. Seyfried, M.S.; Grant, L.E. Temperature Effects on Soil Dielectric Properties Measured at 50 MHz. *Vadose Zone J.* **2007**, *6*, 759–765. [CrossRef]
27. Wharton, R.P.; Hazen, G.A.; Rau, R.N.; Best, D.L. Electromagnetic propagation logging: Advances in technique and interpretation. In Proceedings of the 55th Annual Fall Technical Conference and Exibition of the SPE of AIME, Dallas, TX, USA, 21–24 September 1980.
28. Archie, G.E. The electrical resistivity log as an aid in determining some reservoir characteristics. *Pet. Trans. AIME* **1942**, *146*, 54–62. [CrossRef]
29. Martinsen, O.G. *Bioimpedance and Bioelectricity Basics*, 2nd ed.; House, L., Hill, J., Eds.; Elsevier: Oxford, UK, 2008; pp. 67–68.
30. Vergnano, A. Analysis of Biodegradation of Diesel in Contaminated Soil Using Laboratory Scale Tests. Master's Thesis, Politecnico di Torino, Torino, Italy, 2018.
31. Ministero Delle Politiche Agricole e Forestali. *Metodi Ufficiali di Analisi Chimica del Suolo*; Gazzetta Ufficiale Serie Generale n. 248 (21.10.1999)—Supplemento Ordinario n. 185; Ministero Delle Politiche Agricole e Forestali: Roma RM, Italy, 1999.
32. Turetta, A. Utilizzo di metodi biologici a scala di laboratorio per la bonifica di terreni inquinati da idrocarburi. Master's Thesis, Politecnico di Torino, Torino, Italy, 2017.
33. Palanisamy, N.; Ramya, J.; Kumar, S.; Vasanthi, N.S.; Chandran, P.; Khan, S. Diesel biodegradation capacities of indigenous bacterial species isolated from diesel contaminated soil. *J. Environ. Health Sci. Eng.* **2014**, *12*, 142. [CrossRef]
34. Raffa, C.M. Ottimizzazione delle condizioni chimico-fisiche di un processo di bonifica a supporto del monitoraggio geofisico. Master's Thesis, Politecnico di Torino, Torino, Italy, 2019.
35. Becker, R.; Scheuermann, A.; Schlaeger, S.; Huebner, C.; Wagner, N. Spatial Time Domain Reflectometry (Spatial TDR)—Principles, limitations and accuracy. In *Unsaturated Soils: Advances in Geo-Engineering*; Toll, D.G., Augarde, C.E., Gallipoli, D., Wheeler, S.J., Eds.; © Taylor & Francis Group: London, UK, 2008; ISBN 978-0-415-47692-8.
36. Schnurer, J.; Rosswall, T. Fluorescein Diacetate Hydrolysis as a Measure of Total Microbial Activity in Soil and litter. *Appl. Environ. Microbiol.* **1982**, *43*, 1256–1261.
37. Adam, G.; Duncan, H. Development of a sensitive and rapid method for the measurement of total microbial activity using fluorescein diacetate (FDA) in a range of soils. *Soil Biol. Biochem.* **2001**, *33*, 943–951. [CrossRef]
38. Environmental Protection Agency. *Method 3546 "Microwave Extraction"*; Environmental Protection Agency: Georgetown, Guyana, 2007.
39. Environmental Protection Agency. *Method 8015 "Nonhalogenated Organics Using GC/FID"*; Environmental Protection Agency: Georgetown, Guyana, 2003.
40. Atekwana, E.A.; Atekwana, E.; Legall, F.D.; Krishnamurthy, R.V. Field evidence for geophysical detection of subsurface zones of enhanced microbial activity. *Geophys. Res. Lett.* **2004**, *31*, l23603. [CrossRef]

41. Hiebert, F.K.; Bennett, P.C. Microbial Control of Silicate Weathering in Organic-Rich Ground Water. *Science* **1992**, *258*, 278–281. [CrossRef] [PubMed]
42. Olchawa, A.; Kumor, M. Time Domain Reflectometry (TDR)—Measuring Dielectric Constant of Polluted Soil to Estimate Diesel Oil Content. *Arch. Hydro Eng. Environ. Mech.* **2008**, *55*, 55–62.